

1 **GreenPRO: A novel fertilizer-driven osmotic power generation**
2 **process for fertigation**

3 F. Volpin^{1,§}, R. Gonzales^{1,§}, S. Lim¹, N. Pathak¹, S. Phuntsho^{1, **}, and Ho Kyong Shon^{1,*}

4

5 ¹ School of Civil and Environmental Engineering, University of Technology, Sydney (UTS),
6 City Campus, Broadway, NSW 2007, Australia

7

8

9

10

11

12

13

14

15

16

17

18 [§] F.V. and R.G. equally contributed to this work.

19 ^{*} Corresponding author: Tel.: (+61) 02 9514 2629; email: Hokyong.Shon-1@uts.edu.au

20 ^{**} Corresponding author: Tel.: (+61) 04 2264 5628; email: Sherub.Phuntsho@uts.edu.au

21 **Abstract**

22 This study introduces and describes GreenPRO, a novel concept involving fertiliser-
23 driven osmotic energy generation via pressure retarded osmosis (PRO). The potential of
24 GreenPRO was proposed for three objectives: (a) power generation, (b) water pressurization
25 for fertiliser-based irrigation, and (c) water treatment, as a holistic water-energy-food nexus
26 process. Three pure agricultural fertilisers and two commercial blended fertiliser solutions were
27 used as the draw solution and irrigation water as feed to test this concept for power generation.
28 Theoretical thermodynamic simulation of the maximum extractable Gibbs energy, was first
29 performed. After which, a series of bench-scale experiments were conducted to obtain realistic
30 extractable energy data. The results showed that concentrated fertilisers potentially have 11
31 times higher energy than seawater. Even after accounting for the irreversibility losses due to
32 constant pressure operation, the investigated pure fertilisers were found to have between 2.5 –
33 4.6 Wh/kg of energy. The outcomes from the flux and power density modelling were then
34 validated with real experimental data. This study has successfully demonstrated that
35 concentrated fertilisers can release a substantial amount of chemical potential energy when
36 diluted for fertigation. This energy could be harnessed by transforming it into electric energy
37 or pressure energy via PRO.

38

39 **Keywords:** Pressure Retarded Osmosis; Fertigation; GreenPRO; Salinity Power.

40 **1 Introduction**

41

42 The exponential increase in the world population and urbanization leads to alarming
43 crises in global water scarcity, energy availability, and food security. These could potentially
44 affect global economies. Thus a surge in interest in energy-water-food nexus research and
45 scientific discovery is seen in recent years as a response to optimise the use of water and energy
46 resources to provide food [1]. Water-energy-food nexus is a concept mostly used when
47 sustainable development is discussed, providing a holistic approach to examine the demands
48 of a growing society and how these demands are met.

49 Water and energy are highly essential in ensuring global food supply, through agriculture.
50 The agriculture sector is one of the largest consumers of the world's total fresh water supply,
51 with over 70% of fresh water supply consumed for agriculture alone [2]. Furthermore, food
52 production consumes more than a quarter of the total global energy, and around 90% of global
53 energy production requires water [3, 4]. Agricultural chemicals, such as fertilisers, are
54 important indirect energy inputs in agriculture and food production; in fact, global fertiliser
55 consumption has increased exponentially over the past five decades [4]. It was reported that,
56 from 2015 to 2018, the global demand for nitrogen-, phosphorus-, and potassium-based
57 fertilisers increase 1.8% annually [5]. These fertilisers make up to around 60% of the fertilisers
58 used on-farm for high yield crop production. The continuous global nutrient requirement is
59 expected to affect both raw material availability, as well as greenhouse gas emissions and
60 eutrophication [6]. One of the forms by which nitrogen is delivered through fertilisers is
61 ammonia (NH_3). Approximately 2% of the world energy consumption is used for producing
62 ammonia (NH_3) fertiliser by Haber-Bosch process that required very high temperature and
63 pressure [7, 8], and this process also produces significant amount of carbon dioxide (CO_2) as a
64 by-product. The production of a certain amount of NH_3 leads to the two- to three-fold
65 production of CO_2 as a by-product [8, 9]. NH_3 production alone contributes to 0.93% of the
66 greenhouse gas emission worldwide [8].

67 As irrigation water quality is not always available for agriculture, desalination of
68 seawater and saline aquifers is currently employed through a number of technologies, which
69 include thermal distillation and membrane-based processes [10]. The conventional membrane-
70 based process, reverse osmosis (RO) is an energy-intensive process. Thus the large-scale

71 implementation of RO to provide fresh water supply for agricultural consumption can be costly.
72 This leads to the exploration of other less energy-intensive processes for seawater desalination,
73 such as forward osmosis (FO) and pressure retarded osmosis (PRO). FO and PRO are both
74 osmotically-driven process, such that these utilize the osmotic pressure difference between two
75 streams of different osmotic potential or concentrations separated by a semipermeable
76 membrane to desalinate water of high salinity [11]. Aside from desalination, PRO also uses the
77 chemical potential for osmotic power generation, wherein the osmotic energy obtained between
78 the two solutions is converted into mechanical energy through a water turbine [12, 13].

79 One of the challenges in osmotically-driven processes is the separation and recovery of
80 the highly concentrated draw solution from the desalinated water. Desalination is mainly reliant
81 on the efficiency of draw solution recovery and separation unless there is no need to separate
82 and recover the draw solution. This was the concept of the fertiliser-driven FO (FDFO) process,
83 which was primarily applied for agricultural purposes via fertilised irrigation, or fertigation,
84 wherein the fertilisers are supplied through an irrigation network system. While this process
85 has yet to be fully commercialized, the concept of FDFO has since been the subject of a number
86 of extensive work on fertigation, osmotically-driven processes, and hydroponics [14-23].

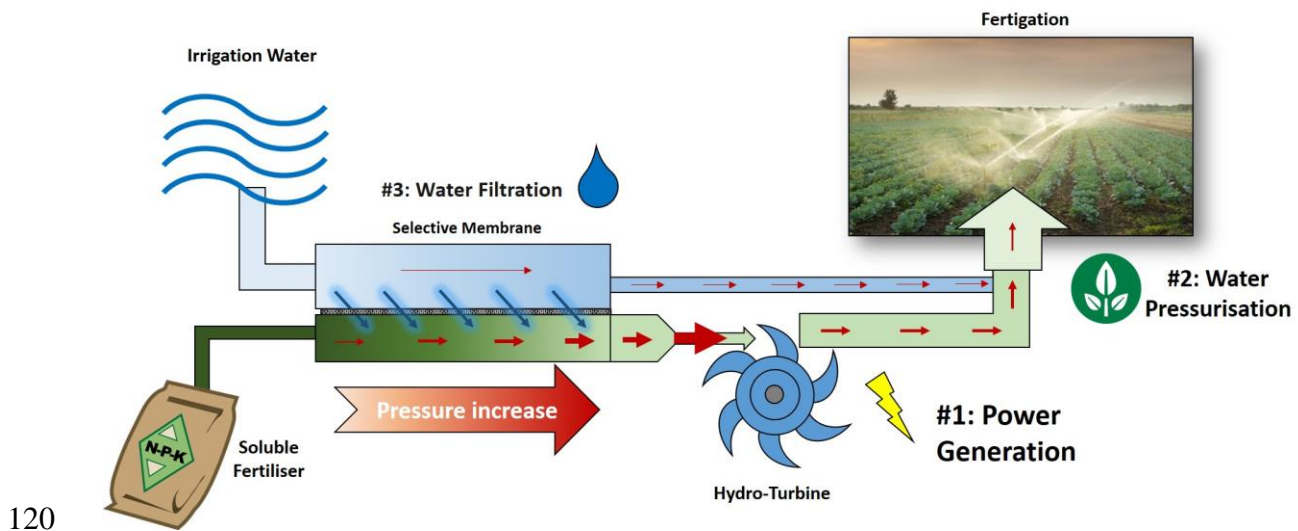
87 Hydroponics, or greenhouse farming, is an agricultural system which maintains a
88 controlled environment suitable for cost-effective and profitable crop production [24]. This
89 particular method, also known as protected cultivation, is advantageous over open field
90 agriculture due to its self-reliance and robustness, such that food production is ongoing
91 throughout the year, unaffected by heavy rainfall, wind, and other anthropological conditions.
92 Opting for greenhouse-based agriculture can potentially save a large amount of fresh water and
93 fertiliser compared to open field agriculture, but this process would entail higher energy
94 requirements. Such high energy requirements may not possibly be met by electrical power
95 supply, especially for rural farms; thus, a need for a decentralized, and possibly, off-the-grid,
96 energy supply in farms arises with the emergence of efficient agriculture practices. This then
97 leads us to the novel combination of fertigation via FDFO and osmotic power generation using
98 PRO, in a process, we call GreenPRO.

99 GreenPRO aims to harvest the Gibbs free energy of mixing between concentrated
100 fertilisers and irrigation water for fertigation to obtain situ generation of useful energy while
101 performing water purification simultaneously. GreenPRO is therefore a perfect example of the
102 water-energy-food nexus concept, having a process wherein water is desalinated, and fertiliser

103 is delivered for irrigation while producing energy at the same time. Through this process,
104 concentrated fertilisers are used as the draw solution to extract pure water from the feed
105 solution and produce electric or potential energy. If irrigation-quality water is used as feed
106 solution, (i) membrane fouling is not expected to significantly reduce the process performances
107 and (ii) the loss of nutrients due to reverse fertiliser diffusion, and optimal fertiliser dilution are
108 not a concern as the concentrated feed can be merged with the partially diluted draw. On the
109 other hand, if impaired water sources are used, this process is expected to suffer the same
110 limitations as FDFO. In that case, the system could be coupled with other treatment processes,
111 such as RO, to provide the remaining water. In such a system, a pressure exchanger could be
112 used to harness the energy generated by the GreenPRO to power the RO. This, however, has
113 to be validated in future studies.

114 In this study, a theoretical analysis of the maximum extractable Gibbs free energy from
115 commercially available agricultural chemicals was initially performed. The theoretical
116 investigation was then backed up by experiments using single and blended commercial
117 fertilisers under different operating conditions. Finally, the outcomes were used to outline the
118 opportunities and challenges of GreenPRO, as well as suggesting future research.

119 2 Methodology



120
121 **Figure 1 Conceptual design of the GreenPRO process.**

122 2.1 Process descriptions

123 Figure 1 shows the whole concept of the GreenPRO process. Irrigation water and
124 fertiliser solution are used as the feed solution and draw solution, respectively. The two
125 solutions are separated by a selective and semi-permeable PRO membrane, whose active layer
126 faces the draw solution (i.e., AL-DS, PRO mode). The osmotic gradient between the two
127 solutions will allow the permeation of water to the draw channel, whose volume is fixed,
128 thereby causing an increase in pressure. The hydraulic pressure build-up in the draw channel
129 can then be transformed into electric energy, via a hydro turbine, or used deliver the pressurised
130 fertigation water to the crops. Similar to FDFO, draw solution recovery is not performed in
131 this process, as it is mixed with the irrigation water stream for direct fertigation. If water
132 treatment is not targeted, the economic impact of reverse nutrient diffusion is also negligible
133 as the concentrated feed solution can be merged with the diluted draw to reach full draw
134 dilution and to close the nutrients mass balance.

135

136 2.2 Specific energy extractable from fertilisers

137 The thermodynamic extractable energy upon the mixing of two solutions with different
138 salinity is extensively investigated and reported in the literature, for the dilution of seawater/RO
139 brine with river water/wastewater [25-27]. In this work, however, the extractable Gibbs free

140 energy of mixing is investigated for the dilution of blended fertilisers or pure agricultural
 141 chemicals with fresh water for irrigation. To fully elucidate the theoretical maximum
 142 extractable energy from concentrated fertilisers, a thermodynamic analysis is required.

143 The Gibbs free energy of mixing per volume of total mixed solution, i.e. ΔG_V , was
 144 calculated using Eq. 1 and 2 [25]:

$$\frac{\Delta G_V}{vRT} = c_M \ln(c_M) - \phi c_F \ln(c_F) - (1 - \phi) c_D \ln(c_D) \quad (1)$$

$$\pi(c) = vRTc \quad (2)$$

145 where the concentration of feed (c_F), draw (c_D) and a mixed solution (c_M) are used. The feed
 146 volume fraction (ϕ) can be approximated by the quotient of the initial feed volume and the
 147 initial volume of the mixing solution $\left[\phi_i = \frac{(V_{D,i} - V_{D,i-1})}{V_{D,i}} \right]$ [25]. In Eq. 2, v is the van't Hoff
 148 factor for strong electrolytes, R is the ideal gas constant, and T is the absolute temperature. By
 149 combining Eq. 1 and 2, ΔG_V can be obtained as a function of the osmotic pressure of the mixing
 150 solutions.

151 For this study, several simplifications of these equations were made. First, it was assumed
 152 that the osmotic pressure $\pi(c)$ follows the van't Hoff equation (Eq. 2). Also, the feed and draw
 153 were assumed to behave like an ideal solution, whose activity coefficient is unity and solute
 154 effect contribution on the volume is negligible [26]. Lin et al. showed that for seawater/river
 155 water or RO brine/river water mixing, this simplification caused a ΔG_V overestimation of less
 156 than 10%. It should be noted, however, that in the case of highly concentrated fertiliser
 157 solutions, the van't Hoff equation is expected to overestimate the real osmotic pressure of the
 158 solution, which might also not behave ideally. To cope with this, an experimental investigation
 159 was also performed in this work.

160 The maximum specific energy extractable from the fertiliser can, therefore, be obtained
 161 by solving the equation $d(\Delta G_V)/d\phi=0$. The result is shown in Eq. 3.

$$\Delta G_{V,\max} \left[\frac{\text{kWh}}{\text{m}^3} \right] = \frac{\pi_D \pi_F}{\pi_D - \pi_F} (\ln(\pi_D) - \ln(\pi_F)) - \exp \left(\frac{\pi_D \ln(\pi_D) - \pi_F \ln(\pi_F)}{\pi_D - \pi_F} - 1 \right) \quad (3)$$

162 In this work, three pure fertilisers $\text{NH}_4\text{H}_2\text{PO}_4$, KCl , and $(\text{NH}_4)_2\text{SO}_4$, and two commercial
 163 liquid blended fertiliser solutions were used for the analysis. Additionally, NaCl was also
 164 employed as a reference salt. The osmotic pressure of the fertiliser solutions was estimated
 165 using OLI Studio Analyser (Version 9.5, Oli Systems Inc., USA). The OLI Studio Analyser
 166 software uses Eq. 2 to calculate the osmotic pressure of a solution. Equation 4 was used to
 167 calculate the theoretical maximum energy extractable from a solid fertiliser:

$$\Delta G_{s,\max} \left[\frac{\text{Wh}}{\text{Kg}} \right] = \frac{\Delta G_{V,\max}}{C_{D,\max}} \quad (4)$$

168 where $C_{D,\max}$ is the maximum solubility of the pure fertiliser in water at 20°C , or the
 169 concentration of the commercial liquid fertiliser. Table 1 shows the maximum solubility and
 170 relative osmotic pressure of the fertiliser solutions considered in this study. Finally, the
 171 theoretical of extractable energy (SE_{\max}) in a constant-pressure, counter-current membrane
 172 module was also calculated with Eq. 5.

$$\text{SE}_{\max} = \frac{(\pi_D - \pi_F)^2}{4 (\pi_D - \pi_F)} \quad (5)$$

173

174 **Table 1 Maximum solubility and relative osmotic pressure of pure and commercial**
 175 **blended fertilisers. OLI Studio Analyser (Version 9.5, Oli Systems Inc., USA) was used**
 176 **for the estimation of C_D and π_D . The C_D , π_D , and D of commercial liquid fertilisers (Blend**
 177 **A, B) were calculated based on the composition provided by the manufacturer.**

	$C_{D,\max}$ (in H_2O at 20°C) [g/L]	Osm. Pressure, π_D [bar]
$\text{NH}_4\text{H}_2\text{PO}_4$	404	174
KCl	340	227
$(\text{NH}_4)_2\text{SO}_4$	754	275
Blend A	216	95
Blend B	128	66

178

179 2.3 Bench-scale FD-PRO experiments

180 Thermodynamic analysis is a useful tool to investigate the theoretical maximum
 181 extractable energy. However, in reality, PRO membranes are not perfectly selective, and
 182 occurrence of concentration polarisation significantly reduces the actual driving force in the

183 membrane boundary layer. The non-ideal property of commercial membrane would then lessen
184 the real maximum ΔG_{mix} . In order to investigate this, actual PRO experiments with commercial
185 pure and blended fertilisers were performed. The materials used and the experimental protocol
186 are presented in this section.

187

188 2.3.1. Materials

189 Three pure agricultural fertilisers, $\text{NH}_4\text{H}_2\text{PO}_4$, KCl , and $(\text{NH}_4)_2\text{SO}_4$, and two commercial
190 liquid blended fertiliser solutions (Optimum Grow - twin pack hydroponic nutrient) were used
191 in this PRO study. NaCl was also used as the reference draw solute for process standardization.
192 All pure chemicals were obtained from Merck and used as received. The commercial liquid
193 blended fertilisers used in this study were obtained from Fernland Agencies Pty Ltd
194 (Queensland, Australia). This is a hydroponic nutrient solution usually employed in plant
195 nurseries and commercial greenhouses. Their composition can be found in the literature [28].
196 This nutrient solution comes with two parts (i.e., A and B) to be diluted separately and then
197 mixed. De-ionised water was used as feed solution. Commercial PRO thin film composite
198 membrane (Toray Chemical Korea Inc., South Korea) was used as the semipermeable
199 membrane.

200

201 2.3.2. Bench-scale PRO experiments

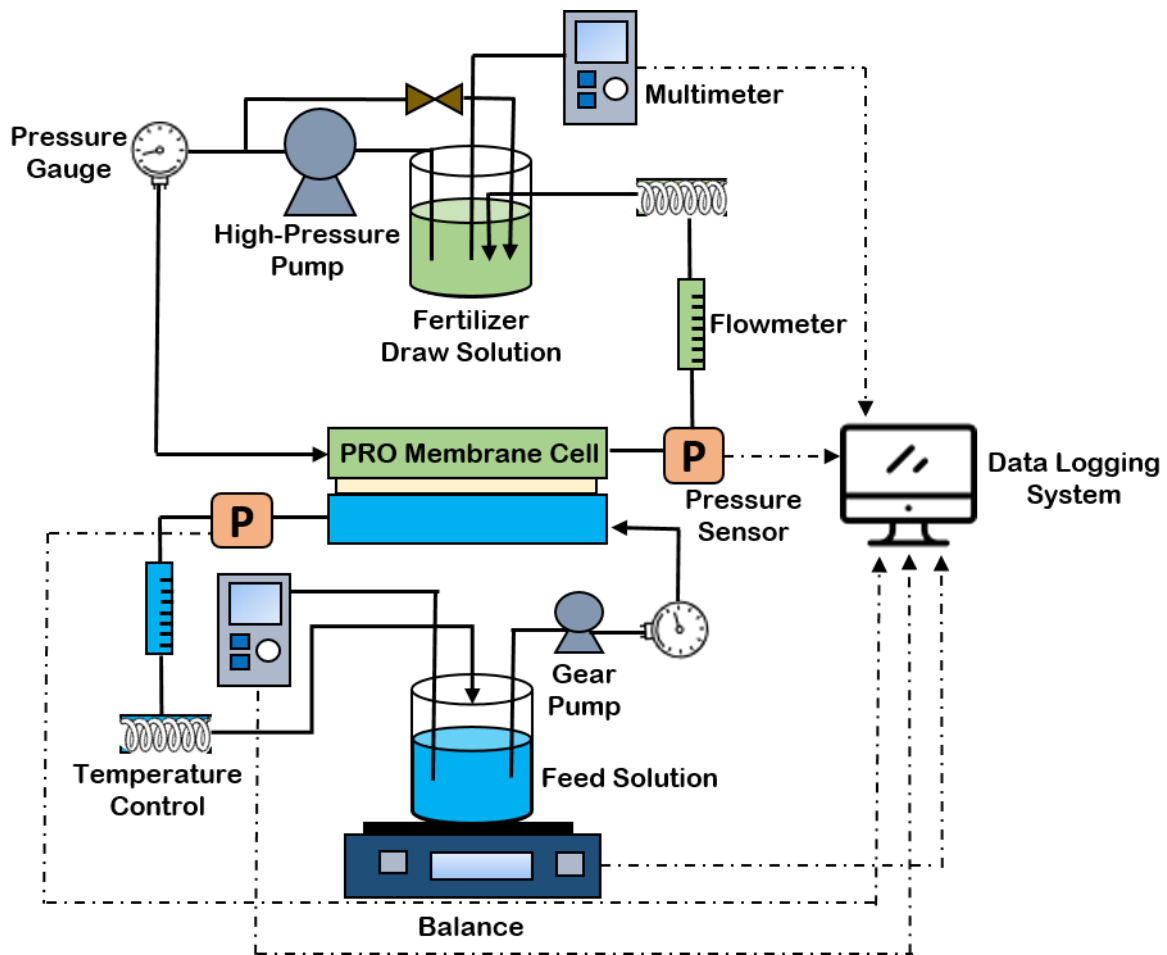


Figure 2 Experimental set-up used for the PRO tests.

The PRO experiments were carried out using a bench-scale system, as shown in Figure 2 (Cheon Ha Heavy Industries Co. Ltd., Gwangju, South Korea). The system consists of stainless-steel based membrane test cell containing two water channels allowing for counter-current operation. A gear pump (Cole Parmer, USA) was used to flow the feed solution while a high-pressure plunger pump (BM-4.18, BTLN, China) was used for the flow and pressurisation of the draw solution. Behind the high pressure pump, the customized buffer chamber (Chunha heavy industry, Republic of Korea) was installed in the PRO unit in order to alleviate the pulsation produced from the pump, so that the applied pressure was constantly maintained under the lab-scale PRO experiments [29]. The channel on the feed solution side had the following dimensions: 77 mm length, 26 mm width, and 2.5 mm depth. The feed solution flowed tangential to the membrane, which had an active area of 20.02 cm². A fixed flow rate of 200 mL min⁻¹ was set for both the draw and feed streams. Mesh spacers were placed on the feed channel to support the membrane. The feed solution was contained in a

218 vessel, whose weight is measured using a top-loading balance (CAS CUW4200HX, CAS,
 219 South Korea) and monitored using the PRO data auto-logging system. The feed solution is
 220 recirculated using a gear pump (Cole Parmer, USA). The draw solution, on the other hand, was
 221 recirculated using a high-pressure positive displacement pump. Conductivity measurements
 222 were monitored by a conductometer (Horiba LAquaact D-74, Horiba Scientific, Japan), while
 223 volume changes of the permeated water and applied pressures were observed and recorded by
 224 the data auto-logging system connected to the lab-scale PRO system.

225 The membrane was firstly stabilized and pre-compacted at 10 bar for 30 min. After pre-
 226 compaction, each fertiliser solutions was tested from 0 bar stepwise till 25 bar (which is the
 227 maximum pressure stated by the manufacturer). All experiments were performed at a fixed
 228 system temperature of 23.0 ± 1.0 °C. The water flux (J_w , $L m^{-2} h^{-1}$) was calculated based on the
 229 permeated volume over time. The power density (W , $W m^{-2}$) was obtained from Eq. 6, where
 230 ΔP is the pressure difference across the PRO membrane [30, 31].

$$W = J_w \cdot \Delta P \quad (6)$$

231 **2.4 Water flux and power density modelling**

232 Water flux and power density of the pure and blended fertilisers were modelled using Eq.
 233 6 and 7, respectively [32, 33].

$$J_w = K \cdot \ln \left(\frac{\pi_D - \left(\frac{J_w}{A}\right) \cdot \left(1 + \left(A \frac{\Delta P}{J_w}\right)\right) + \left(\frac{B}{A}\right) \cdot \left(1 + \left(A \frac{\Delta P}{J_w}\right)\right)}{\pi_F + \left(\frac{B}{A}\right) \cdot \left(1 + \left(A \frac{\Delta P}{J_w}\right)\right)} \right) - \text{AL-DS orientation} \quad (7)$$

234 Eq. 7 specifically accounts for the internal concentration polarisation (ICP) occurring during
 235 the osmotic process, as well as the applied hydraulic pressure. The mass transfer coefficient K
 236 was calculated with Eq. 9 as a ratio of the solute diffusivity D and the structural parameter of
 237 the porous membrane support S [34].

238 The A in eq. 7 value was calculated as the average of the transmembrane flux as a
 239 function of the applied hydraulic pressure, ranging from 5 to 10 bar, i.e. $A = \frac{J_w}{\Delta P}$. To measure
 240 the salt rejection, necessary for the B value calculation (eq. 8), the rejection of a 500 mg/L

241 solution of each salt was measured under 10 bar operating pressure [31]. Finally, the diffusivity
 242 coefficient of each salt was calculated with OLI Studio Analyser (Version 9.5, Oli Systems
 243 Inc., USA). The input data for the modelling can be seen in Table 2.

$$B = \left(\frac{1 - R}{R} \right) \cdot (\Delta P - \Delta \pi) \cdot (A) \quad (8)$$

244 where ΔP is the trans-membrane pressure difference (bar), R the solute rejection and $\Delta \pi$ the
 245 osmotic pressure difference across the membrane.

$$S = \frac{D}{K} \quad (9)$$

246 **Table 2 Input parameters used for the modelling of water flux and power density.**
 247 **Osmotic pressure and diffusivity were estimated using OLI Studio Analyser (Version 9.5,**
 248 **Oli Systems Inc., USA) while rejection, A and S are based on experimental data.**

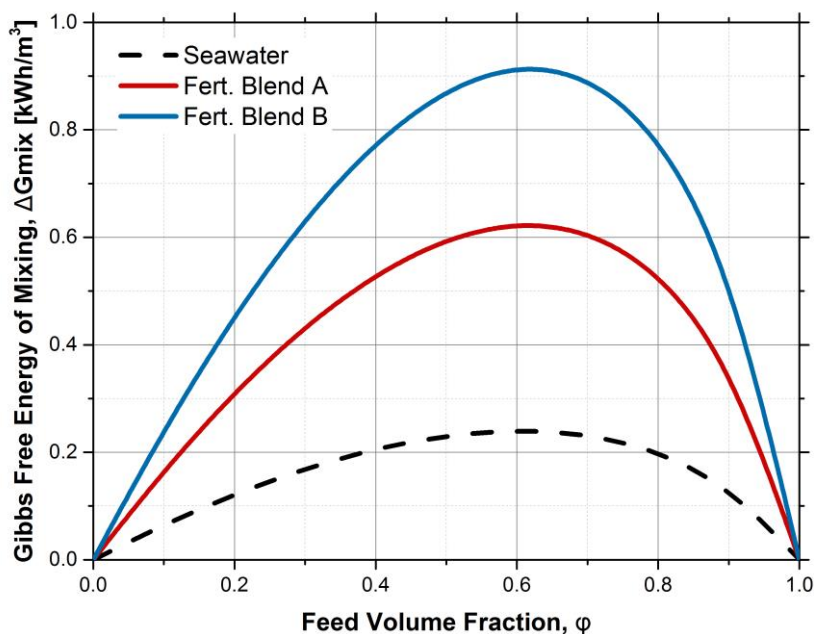
	C_D exp. [M]	Osm. Pressure, π_D [bar]	Diffusivity, D [m ² .s ⁻¹]	Rejection, R [%]	Selectivity, B [L.m ⁻² .h ⁻¹]
NH ₄ H ₂ PO ₄	0.5	22.8	6.70×10^{-10}	97.9	0.84
KCl	0.5	22.3	9.04×10^{-10}	96.4	1.46
(NH ₄) ₂ SO ₄	0.5	24.3	9.45×10^{-10}	97.6	0.96
NaCl	0.6	27.8	1.48×10^{-9}	96.5	1.25
Blend A	As provided	95.2	3.60×10^{-10}	98.1	0.76
Blend B	As provided	66.3	3.60×10^{-10}	98.8	0.46
A [L.m ⁻² .h ⁻¹ .bar ⁻¹]		3.94			
S [μ m]		520			

249
 250
 251 J_w and W were estimated for the concentrated fertiliser solutions using the model, and
 252 the results were first validated with the PRO data from the diluted pure agricultural fertiliser
 253 solutions presented in Table 2. After the validation, the model was used to predict the flux and
 254 power density of the more concentrated commercial liquid fertiliser blends at higher applied
 255 hydraulic pressures.

256 3 Results and Discussion

257 3.1 Maximum Gibbs free energy from single and blended fertilisers

258 A theoretical investigation of the upper limit of the thermodynamic specific extractable
259 energy from the pure and blended fertilisers was first performed. In a thermodynamically
260 reversible system, the applied pressure ΔP variation is always infinitesimally smaller than the
261 osmotic pressure $\Delta\pi$ difference across an ideal perfectly selective and semipermeable
262 membrane [26, 27]. Figure 3 compares the Gibbs free energy, as a function of the feed volume
263 fraction ϕ , of seawater-river water mixing with the energy from mixing commercial liquid
264 fertiliser blends with river water. It can be seen that ΔG_{mix} of the commercial fertilisers is about
265 3.8 times (for Blend A) and 2.6 times (for the Blend B) compared to the ΔG_{mix} of seawater.



266

267 **Figure 3 Comparison of the specific Gibbs free energy of mixing seawater (black, dashed),**
268 **commercial liquid fertilisers blend A, B with river water as a function of the mixing ratio**
269 **of feed and draw (ϕ). Equation 1 was used for the calculation. It was assumed that river**
270 **water has an osmotic pressure of $\pi_r = 0.71$ bar (0.015 M NaCl), seawater has $\pi_{\text{SW}} = 27.84$**
271 **bar (0.6 M NaCl), fertiliser blend A $\pi_{\text{Fert. Blend A}} = 95.2$ bar and fertiliser blend B $\pi_{\text{Fert. Blend B}} = 66.3$ bar.**
272 **The osmotic pressure of the solutions was calculated via OLI Studio Analyser**
273 **(Version 9.5, Oli Systems Inc., USA).**

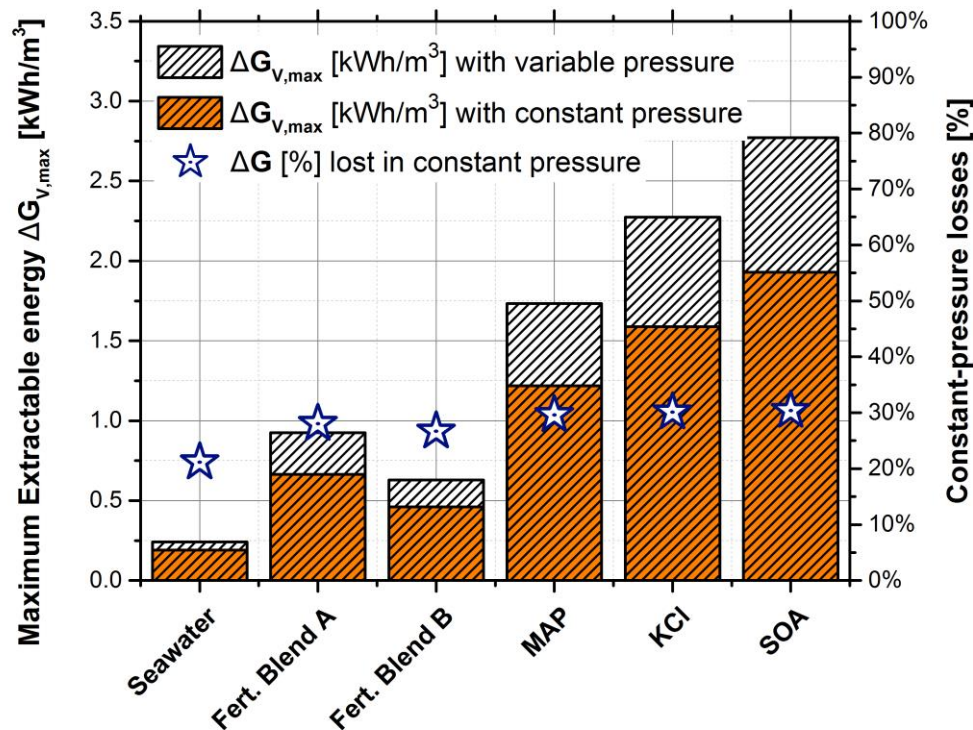
274

275 Nonetheless, in full-scale operation, the GreenPRO system would likely operate under
276 constant pressure, thereby decreasing the maximum extractable energy [27]. In fact, throughout

277 the module, water would permeate from the feed to the draw (i.e., ΔQ); however, this cannot
 278 result in a situation where $\Delta\pi < \Delta P$. Therefore, at constant pressure, there is a limit to the
 279 permeation flow rate ΔQ which results in a lower extractable energy limit $\Delta G_{V, \max}$ [26, 27]. In
 280 a previous study, Straub et al. [35] demonstrated that the countercurrent operation would result
 281 in the maximum theoretical extractable energy limit (Eq. 5).

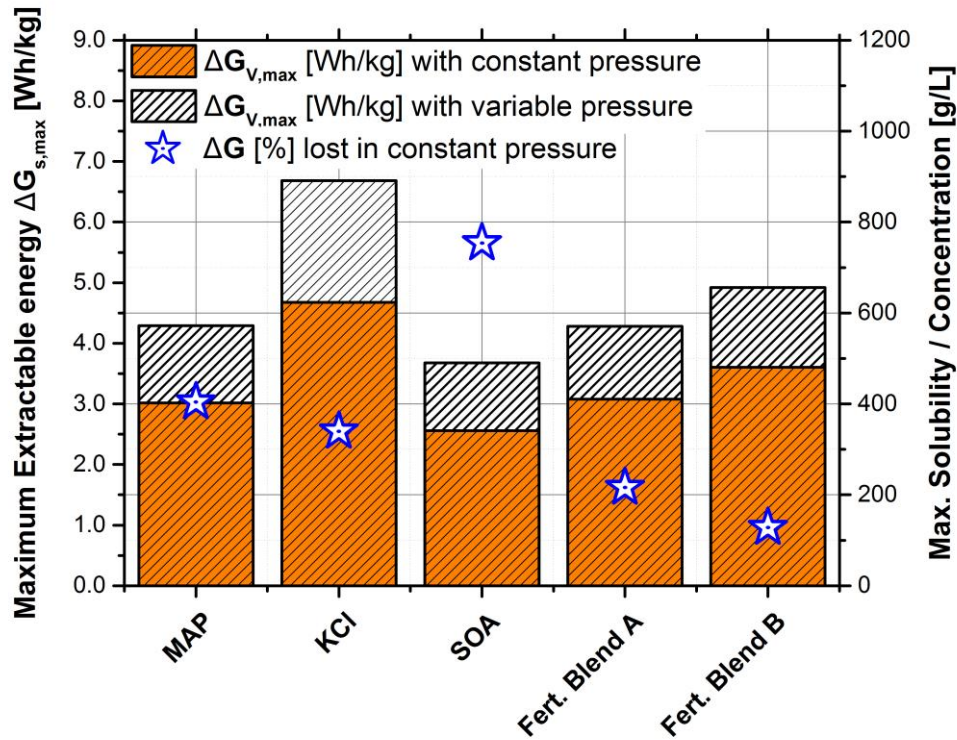
282 By looking at Figure 4, it can be seen that between 20-30% of the specific extractable
 283 energy is lost under constant pressure operation, in accordance with the literature data [27]. It
 284 is also noticeable that pure fertilisers have $\Delta G_{V, \max}$ values considerably higher than that of
 285 seawater. This is because of its high solubility in water that results in very high theoretical
 286 osmotic pressure (i.e., 275 bar for SOA, Table 1). Figure 5 shows that KCl held the highest
 287 $\Delta G_{S, \max}$ due it's high osmotic pressure even at relatively low concentration.

288



289

290 **Figure 4 Comparison between the maximum specific energy $\Delta G_{V, \max}$ of pure fertilisers**
 291 **(eq. 1), at their maximum concentration in water at 20°C, commercial liquid fertiliser**
 292 **blends, and seawater. The losses due to constant-pressure, counter-current mode**
 293 **operation, were accounted for in the orange histogram (eq. 5). The percentage of $\Delta G_{V, \max}$**
 294 **is plotted as blue stars on the right-Y axis. The osmotic pressure of the solutions, used for**
 295 **the calculation, was calculated via OLI Studio Analyser (Version 9.5, Oli Systems Inc.,**
 296 **USA).**



297

298 **Figure 5 Plot of the maximum extractable energy from pure $\text{NH}_4\text{H}_2\text{PO}_4$ (MAP), KCl,**
 299 **$(\text{NH}_4)_2\text{SO}_4$ (SOA), and liquid fertilisers A and B dissolved in water at 20 °C. The losses due**
 300 **to constant-pressure, counter-current mode operation, were accounted for in the orange**
 301 **histogram (eq. 5). Equation 4 was used for the calculation, where $C_{D,max}$ is displayed as**
 302 **blue stars on the right-Y axis. The osmotic pressure of the solutions, used for the**
 303 **calculation, was calculated via OLI Studio Analyser (Version 9.5, Oli Systems Inc., USA).**

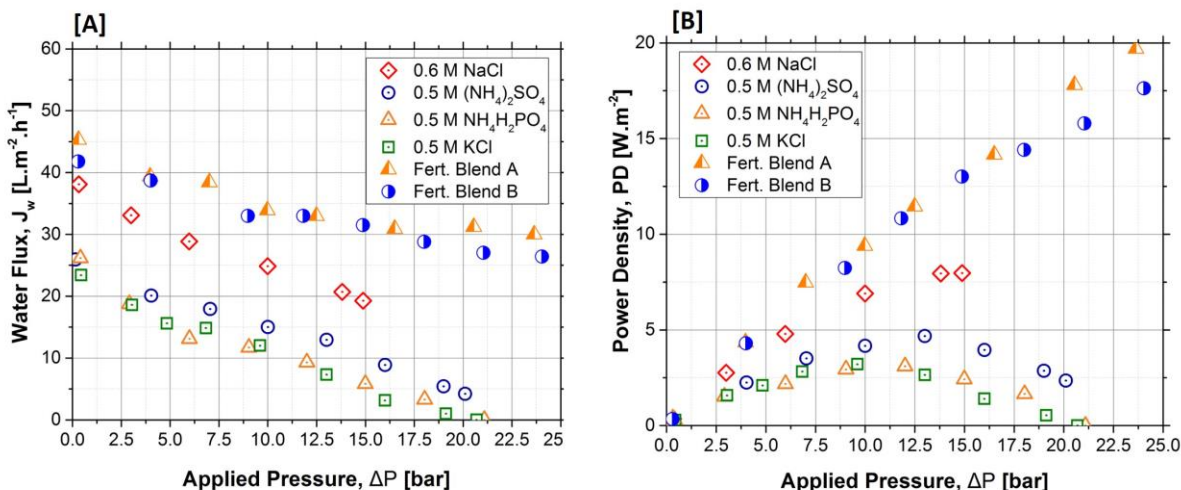
304

305 Based on the specific maximum extractable energy modelling, it can be concluded that
 306 soluble fertilisers held an energy of mixing ranging from 3.7 – 6.7 Wh/kg. This is because of
 307 their high solubility and speciation. This is particularly true for the pure fertilisers. In the case
 308 of commercial liquid blended fertilisers, as a marketing strategy, the value is lower since the
 309 fertiliser solutions have probably not reached saturated conditions. It can be then considered as
 310 an already partially diluted solution. Therefore, it expected that, when concentrated solutions
 311 are mixed with irrigation water, a maximum of 1.7 – 2.6 kWh/m³ could be extracted. These
 312 values decrease by about 30% when the constant-pressure operation losses are accounted for.
 313 Still, these values are overestimating the actual extractable energy as they assume a perfectly
 314 selective semipermeable membrane with no occurrence of ICP. To account for the losses with
 315 the use of a commercially-available membrane (about an additional 15% in the case of
 316 seawater-river water mixing [27]), a full-scale module analysis should be performed. To lay
 317 the foundation for this future analysis, a model to predict the flux and power density of real

318 commercial fertilisers was developed and validated experimentally. The results are presented
319 in the following sections.

320 3.2 Performances of pure and commercial fertilisers under constant pressure

321 Water flux and power density values were plotted as a function of the applied hydraulic
322 pressure for the fertiliser solutions used in this study, as shown in Figure 6. 0.6 M NaCl, the
323 average seawater concentration [36], was used as the standard draw solution for comparison.
324 The pure agricultural chemicals ($\text{NH}_4\text{H}_2\text{PO}_4$, KCl, and $(\text{NH}_4)_2\text{SO}_4$) were dissolved in 0.5 M
325 aqueous solutions, while the commercial fertiliser blends were used as received. Due to the
326 dilute nature of the pure agricultural chemical solutions, a lower water flux and power density
327 were observed, compared to the seawater-like draw solution standard. The water flux of these
328 solutions was also observed to be similar; at 0 bar, $\text{NH}_4\text{H}_2\text{PO}_4$, KCl, and $(\text{NH}_4)_2\text{SO}_4$ exhibited
329 26.2, 23.4, and 25.9 $\text{L m}^{-2} \text{h}^{-1}$, respectively. On the contrary, since the commercial fertiliser
330 blends were used directly without dilution, the overall concentration was expected to be higher
331 than that of seawater; at 0 bar, fertiliser blends A and B exhibited water flux values of 45.3 and
332 41.8 $\text{L m}^{-2} \text{h}^{-1}$, respectively, compared to seawater's 38.1 $\text{L m}^{-2} \text{h}^{-1}$.



333
334 **Figure 6 Experimental results of the measured water flux [A] and power densities [B]**
335 **achieved with 0.5 M single fertilisers, simulated seawater (0.6 M NaCl) and commercial**
336 **liquid fertiliser blends. Toray PRO membrane was used with an applied hydraulic**
337 **pressure up to 25 bar.**

338

339 It can also be seen in Figure 6 that as the applied hydraulic pressure increases, water flux
340 decreases as well. For the pure agricultural chemical solutions, water flux decreased until
341 reaching zero at approximately 21 bar. Moreover, the power density reached a maximum when

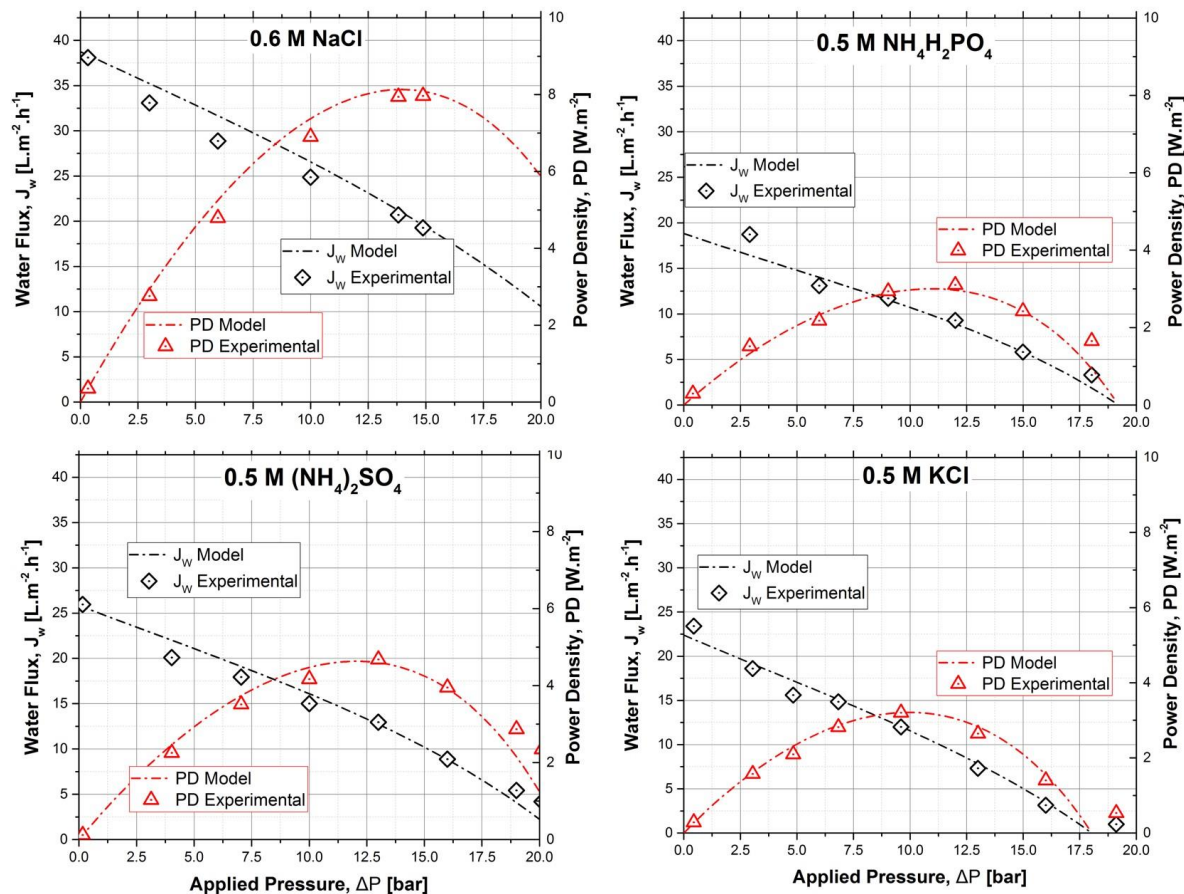
342 the applied hydraulic pressure is approximately half of the pressure at which water flux reaches
343 zero. Maximum power densities of 3.1 W m^{-2} (at 12 bar), 3.2 W m^{-2} (at 9.6 bar), and 4.7 W m^{-2}
344 2 (at 13 bar) for $\text{NH}_4\text{H}_2\text{PO}_4$, KCl , and $(\text{NH}_4)_2\text{SO}_4$, respectively. For the fertiliser blend
345 solutions, sufficient hydraulic pressure to decrease the water flux to 0 was not applied in this
346 study, due to limitations of the bench-scale facility, yet the gradual decrease of water flux and
347 increase of the power density values were observed in this study. During the PRO process, the
348 draw solution is diluted simultaneously as the feed concentration increases. This leads to a
349 reduction of the osmotic pressure gradient between the draw and feed solutions, that, the
350 maximum power density can only be achieved at a certain applied hydraulic pressure value.

351 **3.3 Water flux and power density modelling**

352 Evaluation of the performances of commercial state-of-the-art PRO membranes is
353 essential to estimate the real maximum extractable energy from a fertiliser solution. Straub et
354 al. [27] estimated that approximately 15% of energy loss occurs due to reverse salt flux and
355 concentration polarisation when NaCl is used as draw solution. However, it is clear from Table
356 2 that the diffusivity D (main factor in the ICP effect) and rejection R of fertilisers can differ
357 quite substantially from the diffusivity and rejection of pure NaCl . Thus, the ΔG losses when
358 fertilisers are used as draw solution using a real membrane needs to be evaluated. In this paper,
359 we have focused the attention on the validation of a water flux and power density model to
360 predict the performances of the selected fertilisers. This model can be then used for future
361 analysis of the realistic amount of energy extractable from the concentrated fertiliser solution.

362 Eq. 6 and 7 were used for the calculations, and the input of the equations are displayed
363 in Table 2. Real experimental data were used to validate the modelling results. Figure 7 and
364 Figure 8 show the theoretical and experimental water flux and power density data. It can be
365 seen that even under the assumptions regarding the osmotic pressure and average diffusivity,
366 the model was able to predict closely the flux and power density of liquid commercial fertiliser
367 blends. Figure 8 shows that, theoretically, the high osmotic pressure of the fertiliser blends can
368 lead to power densities between 24 to 29.5 W/m^2 however, there is no commercial osmotic or
369 PRO membranes that can withstand hydraulic pressure between 40 to 50 bars and hence this
370 shows the prospects of the need to develop PRO membranes with significantly enhanced
371 mechanical strength compared to the existing osmotic membranes. There is a trade-off between
372 structural parameters (S) and mechanical strength, and increasing the membrane strength can
373 likely result in increasing also the S value which, in turn, could aggravate the ICP effect. This

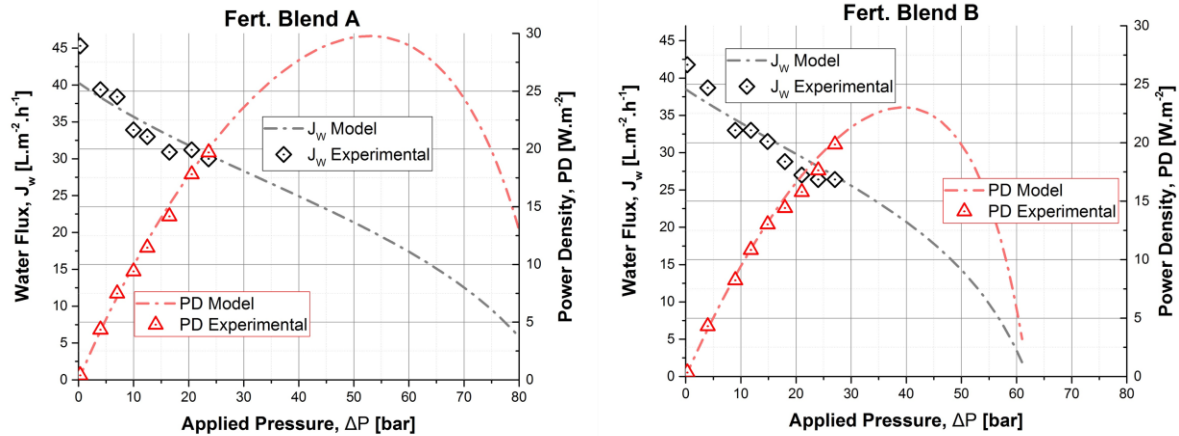
374 therefore opens up opportunities to explore other material composites for improving the
 375 mechanical strength of the PRO membrane without significantly impacting the structural
 376 parameters.



377

378 **Figure 7** Experimental and modelled water flux and power density at different applied
 379 pressures using pure single fertilisers. A 0.6M NaCl solution was also tested and used as
 380 a benchmark. Equations 6 and 7 were used for the calculations, and the input for the
 381 equations are displayed in Table 2.

382



383

384 **Figure 8 Experimental and modelled water flux and power density at different applied**
 385 **pressures using liquid commercial fertiliser blends. Equations 6 and 7 were used for the**
 386 **calculations, and the input for the equations are displayed in Table 2.**

387

388 3.4 Future perspective of GreenPRO

389 In this section, the potential challenges and opportunities for FD-PRO are outlined, and
 390 some research questions are likewise proposed.

391 First, to better understand the realistic amount of extractable energy from fertilisers, a
 392 full-scale module PRO simulation should be performed. This could help in quantifying the
 393 energy losses due to membrane non-ideality [35, 37].

394 Another important investigation is to quantify the amount of fertiliser used by open farms
 395 or greenhouses to understand the volume of draw solution available. This is crucial in
 396 performing a cash flow analysis and calculate the return on investment for a GreenPRO plant.
 397 Additionally, this would also help in understanding how much energy from pump use can be
 398 lowered with this PRO system. Power generation using a hydraulic turbine is, however, not the
 399 only possible application for GreenPRO. In fact, as mentioned in the earlier sections, the
 400 harvested osmotic energy in the form of hydraulic pressure, could be used directly to distribute
 401 the diluted fertiliser to the field, which could effectively reduce the energy expenses for
 402 pumping. Nonetheless, this concept needs to be carefully analysed to understand its viability.
 403 Especially from the engineering point of view, when accounting for the pressure drops during
 404 the process. A combination of power generation, when the fertiliser is highly concentrated, and
 405 water pressurisation, when it is more diluted, could also be investigated to exploit the chemical
 406 energy released during fertiliser dilution fully.

407 As previously mentioned PRO membranes are highly selective toward ions and high
408 molecular weight compound, therefore this process could also be used for simultaneously water
409 purification and power generation, and pressure generation. Brackish water or secondary
410 wastewater effluent could be used as feed solution. In this case, however, the effect of constant
411 pressure in the retention of fertiliser in the draw solution (i.e., reverse salt flux) needs to be
412 carefully evaluated as it might jeopardise the economic feasibility of such process. In fact, one
413 of the advantages in using irrigation water as feed is that the fertiliser lost during reverse
414 permeation during the process can be reintroduced in the diluted draw, thereby ensuring a
415 closed system with no loss of nutrients.

416 Additionally, other salinity gradient processes such as reverse electrodialysis (RED), capacitive
417 mixing (CapMix) and mixing entropy battery should be investigated as a mean to harness the
418 energy diluting concentrated fertiliser solutions [38-41]

419 To conclude, several research questions still need to be addressed to understand the
420 viability of this new concept. However, if the economics would be found favourable, it could
421 be a new approach to reduce the energy consumption and, possibly, improve water reclamation
422 for decentralised farms or greenhouses.

423 **4 Conclusions**

424 A common practice in agriculture is to dilute soluble fertilisers to produce a nutrient
425 solution able to supply both the water and nutrient needs for plants. In the dilution process, a
426 large amount chemical potential energy (i.e., osmotic potential energy) is produced due to the
427 high concentration gradient between the fertiliser salt solution and the irrigation water. In this
428 work, pressure retarded osmosis (PRO) was proposed as a means to harness this chemical
429 potential energy and transform it into electric or pressure energy, through a novel process
430 known as GreenPRO.

431 The thermodynamic maximum Gibbs free energy of mixing single or blended fertiliser
432 salts with irrigation water was initially investigated. The results show that concentrated
433 fertilisers, such as $(\text{NH}_4)_2\text{SO}_4$ or KCl, can reach $\Delta G_{V,\text{max}} > 2 \text{ kWh}\cdot\text{m}^{-3}$, which can be over 11
434 times higher than that produced during seawater/river water mixing. Higher energy was also
435 found to be achieved for solutes with higher solubility and speciation. However, these values
436 decrease by about 30% during constant-pressure operation due to thermodynamic
437 irreversibility losses. In order to have a realistic power density value, the non-ideal nature of
438 the available PRO membranes needs to be accounted for. To do so, water flux and power
439 density model, which accounts for concentration polarisation effect and non-ideal solute
440 rejection, was employed. The model was then fed with the characteristics (i.e., A, B, S) of a
441 commercial PRO membrane, as well as the chemical proprieties of the employed fertilisers,
442 and then validated with real experimental data. The model proved to converge closely to flux
443 values similar to the experimentally measured ones. Based on these data, a full-scale simulation
444 can be later investigated to assess the realistic extractable energy from commercial pure or
445 blended fertilisers.

446 Future efforts should be directed in understanding the economic feasibility of this concept
447 by coupling the measurements of the extractable energy and power density from concentrated
448 fertilisers with the amount of fertilisers normally used in agriculture. This way, a realistic cash
449 flow analysis can be performed.

450 Finally, this study showed the potential of GreenPRO in harnessing fertiliser potential
451 energy for fertigation water pressurisation and/or water treatment. This would hopefully
452 augment high energy requirements typical for most agricultural processes.

453 **Acknowledgements**

454 This research was supported by the Australian Research Council (ARC) through Future
455 Fellowship (FT140101208) and UTS Chancellor's postdoctoral research fellowship.

456

457 **References:**

- 458 [1] E.M. Biggs, E. Bruce, B. Boruff, J.M.A. Duncan, J. Horsley, N. Pauli, K. McNeill, A. Neef, F. Van
459 Ogtrop, J. Curnow, B. Haworth, S. Duce, Y. Imanari, Sustainable development and the water–energy–
460 food nexus: A perspective on livelihoods, *Environmental Science & Policy*, 54 (2015) 389-397.
- 461 [2] W.A. Jury, H. Vaux, The role of science in solving the world's emerging water problems,
462 *Proceedings of the National Academy of Sciences of the United States of America*, 102 (2005) 15715.
- 463 [3] W.W.W.A. Programme), The United Nations World Water Development Report 4: Managing Water
464 under Uncertainty and Risk, UNESCO, Paris, 2012.
- 465 [4] S. Khan, M.A. Hanjra, Footprints of water and energy inputs in food production – Global
466 perspectives, *Food Policy*, 34 (2009) 130-140.
- 467 [5] FAO, World fertilizer trends and outlook to 2020, Food and Agriculture Organization of the United
468 Nations (FAO), (2017) 66.
- 469 [6] United Nations, World Population Prospects: The 2017 Revision, Key Findings and Advance
470 Tables, in: P.D. Department of Economic and Social Affairs (Ed.), 2017, pp. Working Paper No.
471 ESA/P/WP/248.
- 472 [7] D.E. Canfield, A.N. Glazer, P.G. Falkowski, The Evolution and Future of Earth's Nitrogen Cycle,
473 *Science*, 330 (2010) 192-196.
- 474 [8] Y. Bicer, I. Dincer, G. Vezina, F. Raso, Impact Assessment and Environmental Evaluation of
475 Various Ammonia Production Processes, *Environmental Management*, 59 (2017) 842-855.
- 476 [9] A.R. Khan, L. Al-Awadi, M.S. Al-Rashidi, Control of ammonia and urea emissions from urea
477 manufacturing facilities of Petrochemical Industries Company (PIC), Kuwait, *Journal of the Air &
478 Waste Management Association*, 66 (2016) 609-618.
- 479 [10] M.A. Shannon, P.W. Bohn, M. Elimelech, J.G. Georgiadis, B.J. Marinas, A.M. Mayes, Science
480 and technology for water purification in the coming decades, *Nature*, 452 (2008) 301-310.
- 481 [11] M.J. Park, R.R. Gonzales, A. Abdel-Wahab, S. Phuntsho, H.K. Shon, Hydrophilic polyvinyl
482 alcohol coating on hydrophobic electrospun nanofiber membrane for high performance thin film
483 composite forward osmosis membrane, *Desalination*, 426 (2018) 50-59.
- 484 [12] Y. Choi, S. Vigneswaran, S. Lee, Evaluation of fouling potential and power density in pressure
485 retarded osmosis (PRO) by fouling index, *Desalination*, 389 (2016) 215-223.
- 486 [13] D.I. Kim, J. Kim, H.K. Shon, S. Hong, Pressure retarded osmosis (PRO) for integrating seawater
487 desalination and wastewater reclamation: Energy consumption and fouling, *Journal of Membrane
488 Science*, 483 (2015) 34-41.
- 489 [14] S. Phuntsho, H.K. Shon, T. Majeed, I. El Saliby, S. Vigneswaran, J. Kandasamy, S. Hong, S. Lee,
490 Blended fertilizers as draw solutions for fertilizer-drawn forward osmosis desalination, *Environmental
491 Science & Technology*, 46 (2012) 4567-4575.
- 492 [15] S. Phuntsho, S. Hong, M. Elimelech, H.K. Shon, Forward osmosis desalination of brackish
493 groundwater: Meeting water quality requirements for fertigation by integrating nanofiltration, *Journal
494 of Membrane Science*, 436 (2013) 1-15.
- 495 [16] S. Sahebi, S. Phuntsho, J. Eun Kim, S. Hong, H. Kyong Shon, Pressure assisted fertiliser drawn
496 osmosis process to enhance final dilution of the fertiliser draw solution beyond osmotic equilibrium,
497 *Journal of Membrane Science*, 481 (2015) 63-72.
- 498 [17] J.E. Kim, S. Phuntsho, L. Chekli, S. Hong, N. Ghaffour, T. Leiknes, J.Y. Choi, H.K. Shon,
499 Environmental and economic impacts of fertilizer drawn forward osmosis and nanofiltration hybrid
500 system, *Desalination*, 416 (2017) 76-85.
- 501 [18] J.E. Kim, S. Phuntsho, H.K. Shon, Pilot-scale nanofiltration system as post-treatment for fertilizer-
502 drawn forward osmosis desalination for direct fertigation, *Desalination and Water Treatment*, 51 (2013)
503 6265-6273.
- 504 [19] Y. Kim, L. Chekli, W.-G. Shim, S. Phuntsho, S. Li, N. Ghaffour, T. Leiknes, H.K. Shon, Selection
505 of suitable fertilizer draw solute for a novel fertilizer-drawn forward osmosis–anaerobic membrane
506 bioreactor hybrid system, *Bioresource Technology*, 210 (2016) 26-34.
- 507 [20] Y. Kim, Y.C. Woo, S. Phuntsho, L.D. Nghiem, H.K. Shon, S. Hong, Evaluation of fertilizer-drawn
508 forward osmosis for coal seam gas reverse osmosis brine treatment and sustainable agricultural reuse,
509 *Journal of Membrane Science*, 537 (2017) 22-31.

- 510 [21] V.H. Tran, S. Phuntsho, H. Park, D.S. Han, H.K. Shon, Sulfur-containing air pollutants as draw
511 solution for fertilizer drawn forward osmosis desalination process for irrigation use, *Desalination*, 424
512 (2017) 1-9.
- 513 [22] S. Zou, Z. He, Enhancing wastewater reuse by forward osmosis with self-diluted commercial
514 fertilizers as draw solutes, *Water Research*, 99 (2016) 235-243.
- 515 [23] F. Volpin, L. Chekli, S. Phuntsho, J. Cho, N. Ghaffour, J.S. Vrouwenvelder, H. Kyong Shon,
516 Simultaneous phosphorous and nitrogen recovery from source-separated urine: A novel application for
517 fertiliser drawn forward osmosis, *Chemosphere*, 203 (2018) 482-489.
- 518 [24] Harmanto, V.M. Salokhe, M.S. Babel, H.J. Tantau, Water requirement of drip irrigated tomatoes
519 grown in greenhouse in tropical environment, *Agricultural Water Management*, 71 (2005) 225-242.
- 520 [25] N.Y. Yip, M. Elimelech, Thermodynamic and Energy Efficiency Analysis of Power Generation
521 from Natural Salinity Gradients by Pressure Retarded Osmosis, *Environmental Science & Technology*,
522 46 (2012) 5230-5239.
- 523 [26] S. Lin, A.P. Straub, M. Elimelech, Thermodynamic limits of extractable energy by pressure
524 retarded osmosis, *Energy & Environmental Science*, 7 (2014) 2706-2714.
- 525 [27] A.P. Straub, A. Deshmukh, M. Elimelech, Pressure-retarded osmosis for power generation from
526 salinity gradients: is it viable?, *Energy & Environmental Science*, 9 (2016) 31-48.
- 527 [28] L. Chekli, J.E. Kim, I. El Saliby, Y. Kim, S. Phuntsho, S. Li, N. Ghaffour, T. Leiknes, H. Kyong
528 Shon, Fertilizer drawn forward osmosis process for sustainable water reuse to grow hydroponic lettuce
529 using commercial nutrient solution, *Separation and Purification Technology*, 181 (2017) 18-28.
- 530 [29] S. Lim, M.J. Park, S. Phuntsho, A. Mai-Prochnow, A.B. Murphy, D. Seo, H. Shon, Dual-layered
531 nanocomposite membrane incorporating graphene oxide and halloysite nanotube for high osmotic
532 power density and fouling resistance, *Journal of Membrane Science*, 564 (2018) 382-393.
- 533 [30] C.F. Wan, T.-S. Chung, Energy recovery by pressure retarded osmosis (PRO) in SWRO-PRO
534 integrated processes, *Applied Energy*, 162 (2016) 687-698.
- 535 [31] J.Y. Xiong, Z.L. Cheng, C.F. Wan, S.C. Chen, T.-S. Chung, Analysis of flux reduction behaviors
536 of PRO hollow fiber membranes: Experiments, mechanisms, and implications, *Journal of Membrane
537 Science*, 505 (2016) 1-14.
- 538 [32] Q. She, X. Jin, C.Y. Tang, Osmotic power production from salinity gradient resource by pressure
539 retarded osmosis: Effects of operating conditions and reverse solute diffusion, *Journal of Membrane
540 Science*, 401-402 (2012) 262-273.
- 541 [33] C.F. Wan, T.-S. Chung, Osmotic power generation by pressure retarded osmosis using seawater
542 brine as the draw solution and wastewater retentate as the feed, *Journal of Membrane Science*, 479
543 (2015) 148-158.
- 544 [34] S. Chou, R. Wang, L. Shi, Q. She, C. Tang, A.G. Fane, Thin-film composite hollow fiber
545 membranes for pressure retarded osmosis (PRO) process with high power density, *Journal of Membrane
546 Science*, 389 (2012) 25-33.
- 547 [35] A.P. Straub, S. Lin, M. Elimelech, Module-Scale Analysis of Pressure Retarded Osmosis:
548 Performance Limitations and Implications for Full-Scale Operation, *Environmental Science &
549 Technology*, 48 (2014) 12435-12444.
- 550 [36] K. Gerstandt, K.V. Peinemann, S.E. Skilhagen, T. Thorsen, T. Holt, Membrane processes in energy
551 supply for an osmotic power plant, *Desalination*, 224 (2008) 64-70.
- 552 [37] S. Kook, C.D. Swetha, J. Lee, C. Lee, T. Fane, I.S. Kim, Forward Osmosis Membranes under Null-
553 Pressure Condition: Do Hydraulic and Osmotic Pressures Have Identical Nature?, *Environmental
554 Science & Technology*, 52 (2018) 3556-3566.
- 555 [38] Y. Mei, C.Y. Tang, Recent developments and future perspectives of reverse electrodialysis
556 technology: A review, *Desalination*, 425 (2018) 156-174.
- 557 [39] D. Brogioli, R. Ziano, R.A. Rica, D. Salerno, O. Kozynchenko, H.V.M. Hamelers, F. Mantegazza,
558 Exploiting the spontaneous potential of the electrodes used in the capacitive mixing technique for the
559 extraction of energy from salinity difference, *Energy & Environmental Science*, 5 (2012) 9870-9880.
- 560 [40] M. Tedesco, E. Brauns, A. Cipollina, G. Micale, P. Modica, G. Russo, J. Helsen, Reverse
561 electrodialysis with saline waters and concentrated brines: A laboratory investigation towards
562 technology scale-up, *Journal of Membrane Science*, 492 (2015) 9-20.
- 563 [41] M. Ye, M. Pasta, X. Xie, Y. Cui, C.S. Criddle, Performance of a mixing entropy battery alternately

564 flushed with wastewater effluent and seawater for recovery of salinity-gradient energy, Energy &
565 Environmental Science, 7 (2014) 2295-2300.